Korean J. Chem. Eng., 36(6), 981-987 (2019)
DOI: 10.1007/s11814-019-0279-x

pISSN: 0256-1115
eISSN: 1975-7220

High strength Cu foil without self-annealing prepared by 2M5S-PEG-SPS

Anna Lee*, Myung Jun Kim, Seunghoe Choe***, and Jae Jeong Kim*,†**

*School of Chemical and Biological Engineering, Institute of Chemical Process, Seoul National University, 599 Gwanangno, Gwanak-gu, Seoul 08826, Korea
**Department of Chemistry, Duke University, 124 Science Drive, Box 90354, Durham, North Carolina 27708, United States
***Electrochemistry Department, Surface Technology Division, Korea Institute of Materials Science (KIMS), 797 Changwondaero, Sungsan-gu, Changwon, Gyeongnam 51508, Korea
(*Received 14 January 2019 • accepted 20 April 2019*)

Abstract−Cu foil has widely been used as a current collector for Li ion batteries due to its excellent electrical, mechanical properties and facile fabrication process, but improvement in the properties of Cu foil is necessary for continuous development of the Li ion battery. Thinner and stronger Cu foil is being demanded, and the self-annealing of Cu foil needs to be prevented for effective control of properties as well as higher productivity of the fabrication process. We investigated the effects of three additives, 2-mercapto-5-benzimidazole sulfonic acid (2M5S), polyethylene glycol (PEG), and bis (3-sulfopropyl) disulfide (SPS), on the mechanical properties and self-annealing phenomenon of Cu foil. Cu foil deposited with PEG shows the highest tensile strength and elongation after electrodeposition; however, it experiences severe self-annealing for 48 hrs. On the contrary, 2M5S and SPS reduce the self-annealing phenomenon with their incorporation into Cu film, while the initial mechanical properties are worse than those with PEG. Therefore, combinations of additives are investigated to obtain both higher mechanical properties and excellent resistance against self-annealing. Finally, 10 μm-thick Cu foil having a tensile strength of 673 MPa and an elongation of 2.9% without self-annealing can be fabricated using PEG-2M5S-SPS.

Keywords: Cu Electrodeposition, Cu Foil, Organic Additive, Mechanical Property, Self-annealing

INTRODUCTION

The Li ion battery has widely been used to provide power to various electronic devices, such as laptop computers, cellular phones, electrical vehicles, and portable consumer devices due to its high energy density, high power density, long life, and low self-discharge rate [1-3]. A Li-ion battery consists of two electrodes (active materials for lithiation and delithiation), a current collector, an electrolyte, and a separator [4]. Cu foil has typically been used as the current collector for the anode of the Li ion battery due to its excellent conductivity and low cost. Recently, it has been revealed that a thinner and mechanically more robust current collector is required to meet the demand for highly integrated energy storage devices.

Generally, Cu foil is produced by electrodeposition. In detail, a cylindrical metal drum acting as a working electrode is partially submerged in the electrolyte and rotates during the process. Cu electrodeposition takes place on the immersed metal drum, and the deposited Cu film is then mechanically peeled off from the surface of the metal drum. The properties of the Cu foil can be controlled by changing the electrochemical variables, including current density and applied potential, and by deposition methods such as constant current or potential, pulse or pulse-reverse electrodeposition, rotating speed of metal cylinder, and the composition of electrolyte [5-7]. In particular, the organic additives introduced in the electrolyte critically affect the morphology and mechanical/electrical properties of Cu film [8-11]. For example, it was reported that the addition of benzotriazole (BTA) or thiourea significantly reduces the grain sizes of Cu deposits, thereby improving the mechanical hardness in accordance with the Hall-Petch relation [10,12]. Also, pulse or pulse-reverse electrodeposition can tune the mechanical and electrical properties of Cu film [13-21].

In addition to the properties of Cu foil, the control of self-annealing is also important for improving the mechanical property and fabrication process. Self-annealing is a phenomenon in which changes in the microstructures of electrodeposited Cu occur without any post heat treatment, accompanied with the diffusion of grain boundaries, resulting in an increase in grain size and the development of (200) orientation [22]. Although a decrease in the electrical resistivity due to the grain growth can be a benefit of self-annealing, the loss of initial high strength is one of the limitations to making more robust Cu foil [23-25]. In addition, self-annealing usually lasts for a few hours or several days [26-32], which is significantly longer than the electrodeposition process. The mechanical properties of Cu foils should be stabilized before using them in Li ion battery fabrication. Therefore, the use of produced Cu foils in the fabrication of Li ion battery is delayed until self-annealing finishes. Although an additional thermal annealing process can be adopted to accelerate the change in the properties of Cu foils, this method is not cost-effective for bulk production. Therefore, accelerating or eliminating the self-annealing of Cu foils could increase the productivity of Cu foil and Li ion battery fabrication.

The self-annealing process of electrodeposited Cu films is affected

†To whom correspondence should be addressed.
E-mail: jjkimm@snu.ac.kr

by the thickness of the film and the deposition conditions including electrodeposition modes (constant current, pulse, and pulse-reverse electrodeposition), applied current density, and organic additives [29,33,34]. An increase in the thickness and current density accelerates the self-annealing process [29,35]. However, the effects of organic additives on self-annealing are not simple [35]. Although it is obvious that self-annealing could not occur in the absence of organic additives [35-37], self-annealing can be driven or prevented by incorporating organic additives.

Self-annealing induced by incorporating additives has been explained in terms of the intrinsic instability of as-deposited Cu film due to defect energy, impurity distribution, and stress by organic additives [22,26-32,38]. Lee et al. [28] reported that an incorporated polyethylene glycol (PEG) could create local stress that accelerated the diffusion of the grain boundary. In addition, other studies maintain that the impurities incorporated between grain boundaries are driving forces of self-annealing of Cu by segregation and diffusion [29,32]. It was also reported that the incubation time for self-annealing was linearly increased with the ratio of stress and impurity factors [34].

In contrast, it has been reported that the organic additives containing sulfur or nitrogen atoms, such as 2-mercaptobenzothiazole sodium salt, 2-mercapto-5-benzimidazolesulfonic acid sodium salt dihydrate, and sodium-3-(5-mercapto-1H-tetrazole-1-yl)benzenesulfonate-monohydrate, are able to inhibit self-annealing [33]. Surholt et al. [39] reported that Cu-S complex incorporated in Cu film can act as the second phase particle, which effectively inhibits the motion of grain boundaries. In addition, Matsuda et al. [33] observed that the mercapto group and the functional groups containing nitrogen atoms reduce the self-annealing phenomenon due to the increase in the concentration of incorporated impurities.

Considering the method of controlling the film properties and self-annealing of the Cu deposit, it is reasonable to suggest that the development of an organic additive for Cu electrodeposition is a proper approach to improve the properties of Cu foil as well as to inhibit self-annealing. Therefore, we investigated the effects of PEG, bis (3-sulfoproply) disulfide (SPS), and 2-mercapto-5-benzimidazole sulfonic acid (2M5S) on both the mechanical properties and self-annealing of Cu foil and finally suggested the additive chemistry for the fabrication of Cu foil having excellent mechanical properties without self-annealing.

MATERIALS AND METHODS

The aqueous electrolytes for electroplating basically consisted of 1.4 M $CuSO_4$, 3.1 M H_2SO_4, and 0.85 mM HCl. To compare the effects of additives, either 56 μM SPS, 10 μM PEG (MW=1,000), 243 μM 2M5S or their combinations were added to the electrolyte. In the absence of any additives, Cu electrodeposition took place irregularly and mechanical tests were not feasible. The addition of PEG-SPS is required to obtain smooth Cu foils, and we investigated the effect of 2M5S on the mechanical properties of Cu foils in the presence of PEG and SPS. The temperature of the electrolyte was precisely controlled to 55 °C by using a temperature controller (Temp-air control unit, Jungdo Instruments), and the electrolyte was circulated by a mechanical pump. The electrodeposition was performed in a two-electrode system consisting of a Ti plate having a geometric area of 100 cm^2 as a working electrode and an insoluble IrO_2/Ti plate as a counter electrode. The current density for Cu electrodeposition was fixed at 600 mA/cm^2, and the thickness of the Cu film was controlled to 10 (±0.5) μm.

The tensile properties of electrodeposited Cu foils were analyzed using a universal testing machine (UTM, 5965, Instron) with a 1 kN load cell at a strain rate of 50 mm/min. The measurements were carried out three times, at 0 hr, 24 hrs, and 48 hrs after electrodeposition to investigate the self-annealing phenomenon according to the organic additives. The microstructure of the Cu film was analyzed using a focused ion beam (FIB, VERSA 3D, FEI) combined with a scanning electron microscope (SEM, VERSA 3D, FEI) and X-ray diffraction (XRD, D8 DISCOVER, Bruker). The contents of impurities in Cu foils were acquired using time-of-flight secondary ion mass spectrometry (TOF-SIMS, ION-TOF GmbH, Münster). The sheet resistance of Cu foils was measured by a four-point probe (CMT-SR1000N, Chang Min Tech.).

RESULTS AND DISCUSSION

The true stress-strain curves of the as-deposited Cu foils from single additive (2M5S, PEG, and SPS) are shown in Fig. 1(a), indicating that the mechanical properties of Cu foils significantly differed according to the additives. It was observed that Cu foil de-

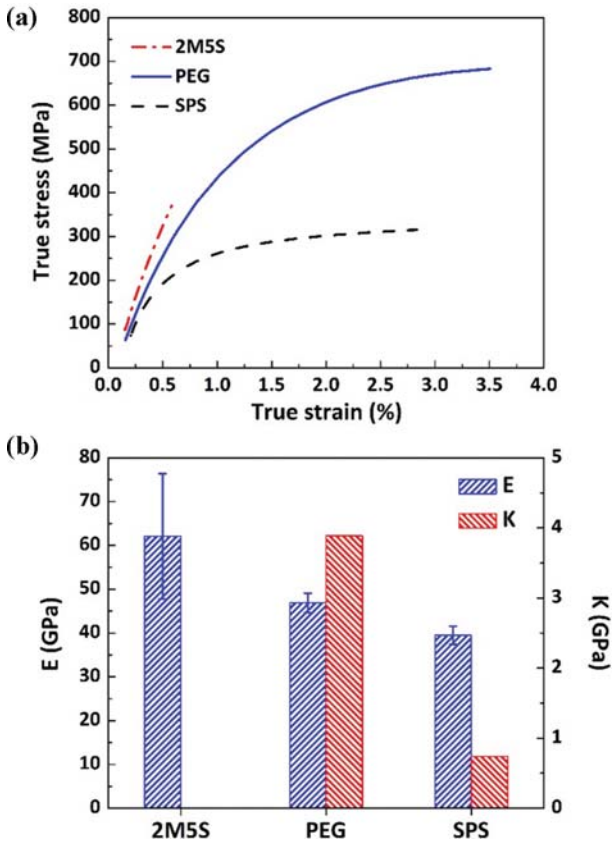

Fig. 1. (a) Stress-strain curves for the Cu foils deposited with SPS, 2M5S, and PEG and (b) the values of E and K calculated from stress-strain curves shown in (a).

posited with PEG was the strongest and the most ductile, with a plastic flow area having a wide range among the three Cu foils. Cu foil from SPS also showed plastic deformation similar to PEG. However, 2M5S resulted in a stress-strain curve with a high slope, indicating high stiffness. Eventually, the Cu foil was torn at small elongation (0.7%) without plastic deformation.

The stress-strain relation during elastic (Eq. (1)) and plastic (Eq. (2)) deformations are given below [40,41].

$$\sigma_T = E\varepsilon_T \quad (1)$$

$$\sigma_T = \sigma_0 + K\varepsilon_T^{0.5} \quad (2)$$

where σ_T is the stress, ε_T is the strain, E is Young's modulus, K is the strength coefficient in the plastic deformation regime, and σ_0 is the constant.

Typical stress-strain curve of metal in a tensile test shows elastic-plastic behavior. At the stress-strain curve, metal initially showed elastic behavior, in which the stress is proportional to strain with a constant slope (Young's modulus), as described in Eq. (1). After passing the critical point, the material experiences plastic deformation until it fractures. This plastic deformation is an irreversible change which can be described by Eq. (2). That is, E and K can describe the mechanical properties of Cu foil in the elastic and plastic deformation regimes, respectively. The tensile strength of Cu foil is the sum of the effects from both elastic and plastic deformation [42-46].

When adding either SPS or PEG alone, the stress-strain curve showed elastic behavior, followed by plastic deformation, which is a typical characteristic of ductile materials. Young's modulus (E) can be obtained from the initial slope of the elastic region, and the strength coefficient (K) is calculated from the plastic deformation region in the stress-strain curve. However, the Cu foil prepared with 2M5S was broken at 0.7% of strain without plastic deformation due to its brittleness; thus, only E can be calculated from Eq. (1).

Fig. 1(b) summarizes the E and K values for the three Cu foils from the aforementioned equations. When using 2M5S, the highest E value (62.1 GPa) was obtained. However, 2M5S increased the brittleness of the Cu foil. Therefore, the tensile strength was the lowest because Cu foil was broken before the plastic deformation. For Cu foil deposited with PEG, a lower E (46.9 GPa) in the elastic deformation regime was obtained; however, the tensile strength was the highest due to the highest K (3.17 GPa). In contrast, both E (39.5 GPa) and K (0.71 GPa) values were relatively low when using SPS, which resulted in the lowest tensile strength (272 MPa). The maximum strain measured at the fracture point was in the order of PEG (3.5%)>SPS (2.8%)>2M5S (0.7%).

While PEG is an additive that renders Cu foil more ductile and stronger, it has been reported that Cu foil prepared with PEG could

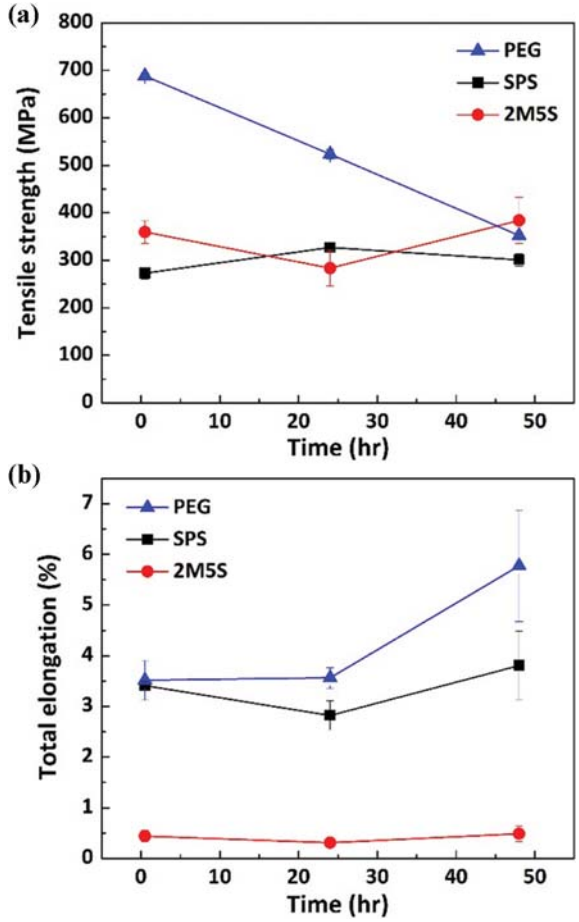

Fig. 2. Time-dependent (a) tensile strength and (b) total elongation of the Cu foils prepared with SPS, 2M5S, and PEG.

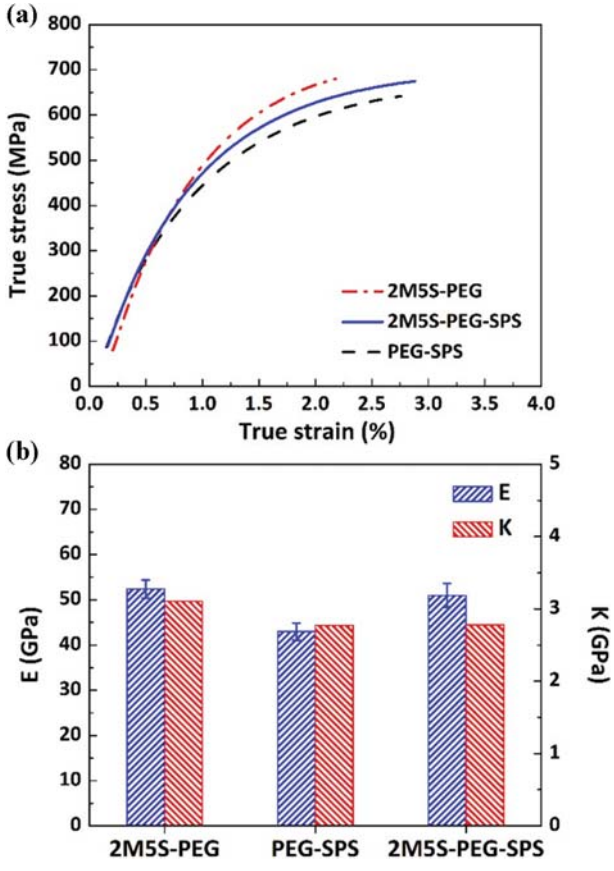

Fig. 3. (a) Stress-strain curves for Cu foils obtained using 2M5S-PEG, PEG-SPS, and 2M5S-PEG-SPS and (b) the values of E and K calculated from stress-strain curves shown in (a).

experience significant self-annealing, which could change the mechanical properties from the as-deposited foil (4). Therefore, the changes in tensile strength and total elongation as a function of shelf time were analyzed. As presented in Figs. 2(a) and 2(b), the Cu foil deposited with PEG experienced severe self-annealing, as evidenced by the drop in tensile strength from 688 MPa to 352 MPa and the simultaneous increase in total elongation from 3.5% to 5.8% after 48 hrs. These results suggest that PEG is inappropriate for the industrial process for the fabrication of Cu foil, as explained above. In contrast, when using either 2M5S or SPS, no significant changes in mechanical properties were observed.

Since the single addition of three additives was not appropriate to fabricate Cu foil with high strength and ductility as well as to prevent self-annealing of Cu foil, combinations of organic additives were applied to the deposition of Cu foils. The true stress-strain curves of as-deposited Cu films obtained from the additive combination are presented in Fig. 3(a). For all combinations, the tensile strength/total elongation were comparable to those for PEG (639 MPa/2.12% for 2M5S-PEG, 627 MPa/2.66% for PEG-SPS, and 654 MPa/2.77% for 2M5S-PEG-SPS).

The E and K of Cu foils from the additive combinations are summarized in Fig. 3(b). The E from the additive combinations was located in the middle of that from the single additive, i.e., 2M5S (62.1 GPa)>2M5S-PEG (52.4 GPa)~2M5S-PEG-SPS (51.0 GPa)> PEG (46.9 GPa)>PEG-SPS (43 GPa)>SPS (39.5 GPa). Similarly, the K values were in the order of PEG (3.17 GPa)>2M5S-PEG (3.06 GPa)>PEG-SPS (2.42 GPa)~2M5S-PEG-SPS (2.44 GPa)>SPS (0.71 GPa). The PEG resulted in high K value and total elongation that were required to obtain high tensile strength. When SPS was combined with PEG, the E, K, and total elongation reduced, leading to the decrease in tensile strength. Compared to PEG-SPS, 2M5S-PEG-SPS showed slightly higher tensile strength because the addition of 2M5S increased E in the elastic deformation regime. Meanwhile, relative to 2M5S-PEG, the 2M5S-PEG-SPS led to higher total elongation, which was probably because SPS further reduced the brittleness of Cu foil caused by 2M5S. In summary, PEG and 2M5S played

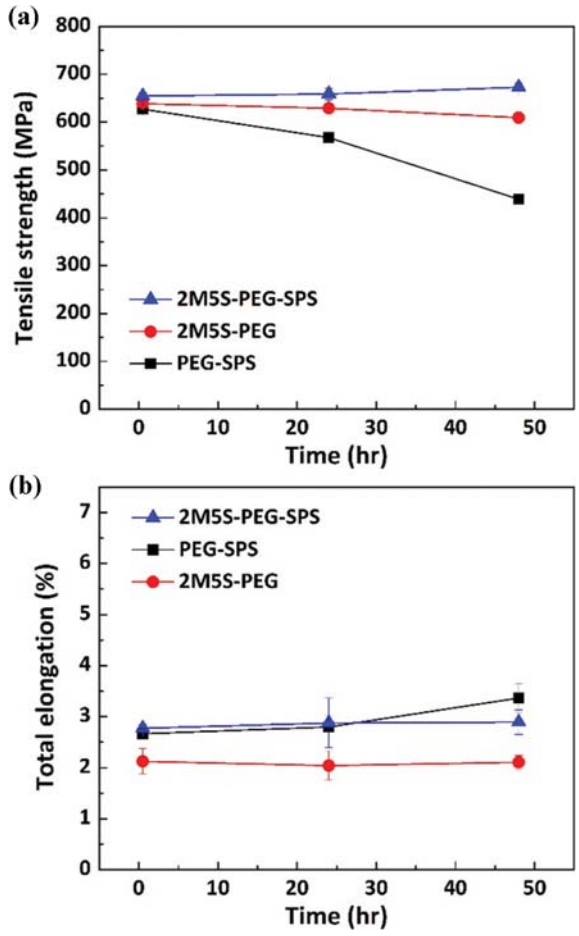

Fig. 4. Time-dependent (a) tensile strength and (b) total elongation of the Cu foils prepared with 2M5S-PEG, PEG-SPS, and 2M5S-PEG-SPS.

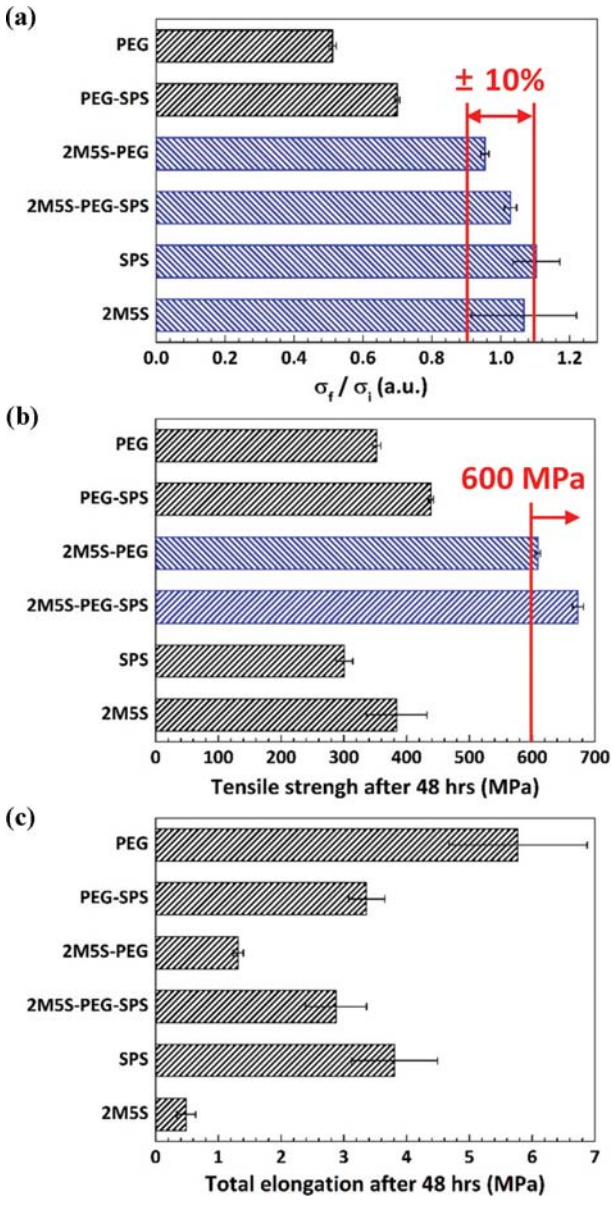

Fig. 5. (a) Ratio of tensile strength before and after self-annealing (σ_f/σ_i), (b) tensile strength and (c) total elongation after 48 hrs according to the additives.

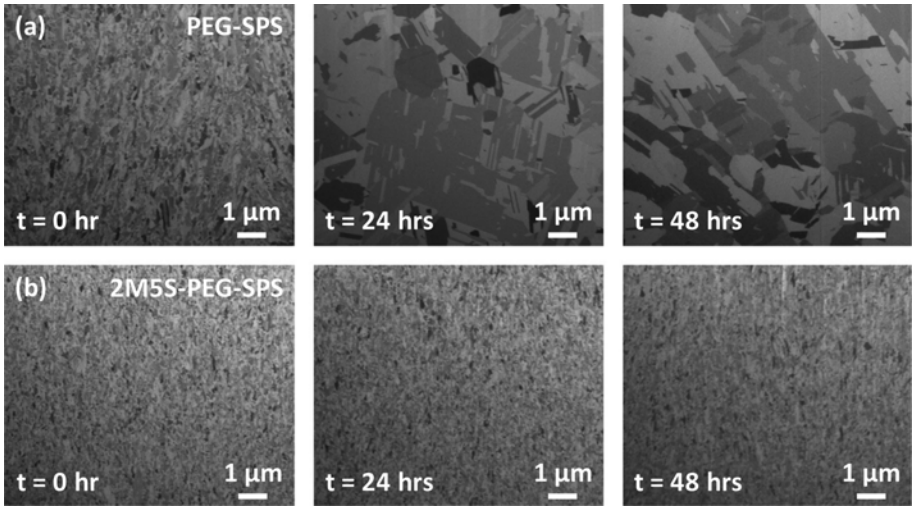

Fig. 6. Cross-sectional images of Cu foils deposited with (a) PEG-SPS and (b) 2M5S-PEG-SPS as a function of self-annealing period.

a role of improving tensile strength by providing high K and E values.

The time-dependent changes in the tensile strength and total elongation of Cu foils obtained with additive combinations are shown in Fig. 4. The 2M5S-PEG and 2M5S-PEG-SPS resulted in negligible changes in tensile properties during 48 hrs. Especially, the Cu foil from 2M5S-PEG-SPS was the most stable against self-annealing (654 MPa to 673 MPa of tensile strength and 2.8% to 2.9% of total elongation after 48 hrs). In contrast, for PEG-SPS, a decrease in tensile strength and increase in total elongation were observed. The extent of self-annealing for various additive combinations is summarized by the ratio of σ_f (tensile strength after 48 hr)/σ_i (initial tensile strength) (Fig. 5(a)). The σ_f/σ_i was close to 1 when using either 2M5S or SPS alone, indicating good stability against self-annealing. This value decreased to 0.51 with PEG. When combining PEG with 2M5S and SPS, this ratio increased to 0.95 and 0.70, respectively. Adding both SPS and 2M5S to PEG further increased σ_f/σ_i to nearly 1, implying negligible self-annealing. These results indicate that 2M5S is the most effective additive for inhibiting self-annealing. SPS also increases the resistance against self-annealing, although it is weaker than 2M5S. Furthermore, we measured the tensile strength of Cu foils deposited with 2M5S after annealing at 130 °C for 10 min. The tensile strength of the annealed Cu foils was almost identical to that of the self-annealed Cu foils (3% difference), also supporting that the incorporated 2M5S effectively inhibited property changes due to the grain growth.

The tensile properties of Cu foils after self-annealing are summarized in Figs. 5(b) and 5(c). While the Cu foil deposited with PEG showed the highest total elongation, this Cu foil underwent severe self-annealing (σ_f/σ_i=0.51). Among the additive combinations showing a property change of less than 10%, 2M5S-PEG-SPS showed the best tensile properties (673 Mpa of tensile strength and 2.9% of total elongation). This improvement of mechanical properties is due to (i) effective inhibition of self-annealing by SPS and 2M5S, (ii) increase in E in elastic deformation regime by 2M5S, and (iii) decrease in brittleness by PEG and SPS enabling Cu foil to undergo large plastic deformation with high K value.

To clarify the effect of 2M5S on the inhibition of self-annealing, we investigated the changes in the grain size, the crystal structure, and the impurity contents of Cu deposits using two representative samples (PEG-SPS and 2M5S-PEG-SPS). Figs. 6(a) and 6(b) show a cross-sectional image of the Cu films deposited with PEG-SPS and 2M5S-PEG-SPS, respectively. In the case of PEG-SPS, the grain size dramatically increased from 115±3 nm (as-deposited) to 782±500 nm (24 hrs) and to 1.2±1 μm (48 hrs). On the contrary, in the presence of 2M5S, the grain growth was strongly restrained (112±31 nm, 118±34 nm, and 112±10 nm at 0, 24, and 48 hrs, respectively). The smaller grains from 2M5S potentially increased the electrical resistance of Cu foils. However, the sheet resistance of Cu foil prepared with 2M5S-PEG-SPS (2.11 mΩ sq^{-1}) was comparable to that from PEG-SPS (2.12 mΩ sq^{-1}). Since the grain size from 2M5S-PEG-SPS was considerably larger than the electron mean free path for Cu at room temperature (39 nm) [18], the effect of grain size on the electrical resistance was negligible for the Cu foils examined in this study.

In addition, the changes in the crystal structure were investigated. XRD patterns for Cu films deposited with PEG-SPS and 2M5S-PEG-SPS are shown in Figs. 7(a) and 7(b). In the case of PEG-SPS, (200) crystal orientation significantly developed after 48 hrs from the electrodeposition, while the (111) peak slightly increased. However, when Cu foil was deposited with 2M5S-PEG-SPS, the crystal structure was much more stable; thus, the intensities of Cu, the (111) and (200) peaks, were almost similar after 48 hrs. The peak intensity ratio shown in Fig. 7(c) summarizes this behavior. The (200)/(111) peak intensity ratio from the case of PEG-SPS continuously increased, while it was constant for 2M5S-PEG-SPS. These results imply that 2M5S assisted the formation of the Cu grains that had the higher resistance against self-annealing; in particular, 2M5S inhibited the development of the (200) orientation in the Cu deposit. As reported by Hasegawa et al. [36], Cu (200) grains grew dominantly during self-annealing due to the smaller strain energy of the (200) orientation than that of the (111) orientation. From Figs. 6 and 7, the addition of 2M5S inhibited the growth of (200) grains, which enabled the mechanical properties of the as-deposited Cu foil to be maintained.

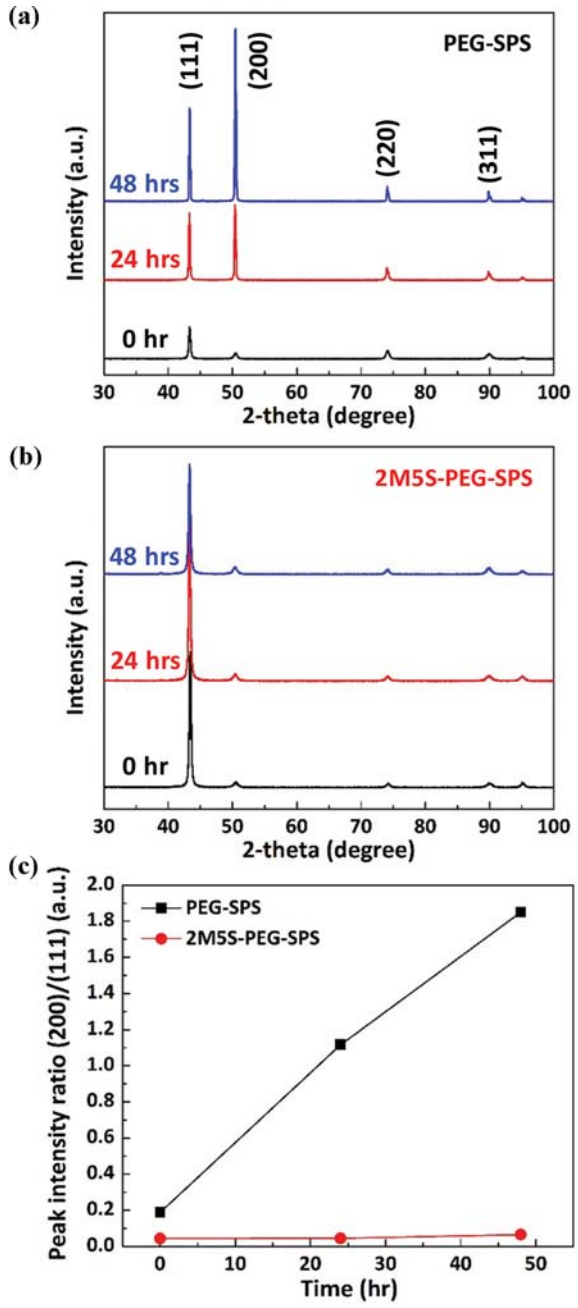

Fig. 7. XRD patterns for Cu foils deposited with (a) PEG-SPS and (b) 2M5S-PEG-SPS as a function of the self-annealing period, and (c) the intensity ratios of (200) and (111) peaks.

As explained above, the incorporation of sulfur in Cu film is important to inhibit self-annealing, and 2M5S was expected to increase the sulfur content in Cu film because it has mercapto and sulfonate groups. Therefore, we compared the sulfur concentrations in Cu foils deposited with PEG-SPS and 2M5S-PEG-SPS using TOF-SIMS (Fig. 8). In the absence of 2M5S (PEG-SPS), the sulfur was detected due to the incorporation of SPS. When using 2M5S-PEG-SPS, the sulfur content was ten-times higher than that using PEG-SPS, implying the additional incorporation of 2M5S. The sulfur atoms at 2M5S could bind with Cu ions, acting as second phase

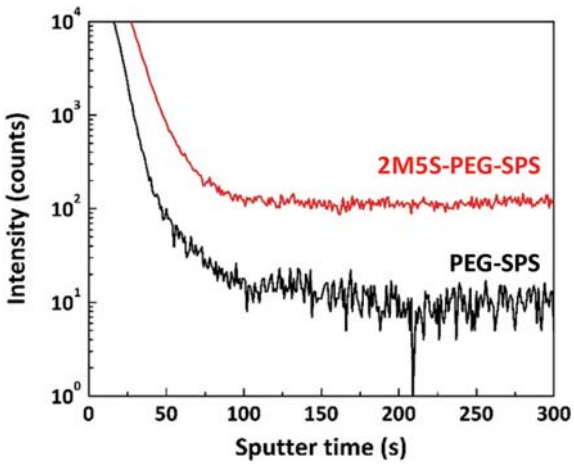

Fig. 8. Contents of incorporated sulfur in Cu foils deposited with PEG-SPS and 2M5S-PEG-SPS.

particles and exert pinning pressure that diminished the grain boundary motion (5). Compared to SPS, 2M5S was more rapidly incorporated during Cu electrodeposition. That is, the increase in the sulfur content in the Cu deposit caused by the incorporation of 2M5S effectively inhibited the self-annealing phenomenon.

CONCLUSIONS

The combination of 2M5S-PEG-SPS was suggested for promising additive chemistry to obtain Cu foil having excellent tensile properties and self-annealing resistance. When PEG was solely used, the Cu foil initially showed very high tensile strength/total elongation; however, it also underwent rapid self-annealing. The incorporation of SPS and 2M5S prevented self-annealing, while the mechanical properties of Cu foils deposited with these additives were worse than with the incorporation of PEG. Especially, 2M5S effectively inhibited the development of (200) orientation and grain growth during self-annealing. Based on the synergetic effect of PEG, SPS, and 2M5S, more robust and ductile Cu foil was obtained with negligible self-annealing, which can shorten the production time for Cu foil.

ACKNOWLEDGEMENTS

This work was supported by the Technology Innovation Program (10043789) funded by the Ministry of Knowledge Economy (MKE, Korea). It was also supported by the National Research Foundation of Korea (NRD) grant funded by the Korea government (MIST) (2019R1A2C1002400).

REFERENCES

1. B. Scrosati and J. Garche, *J. Power Sources*, **195**, 2419 (2010).
2. V. Etacheri, R. Marom, R. Elazari, G. Salitra and D. Aurbach, *Energy Environ. Sci.*, **4**, 3243 (2011).
3. L. Lu, X. Han, J. Li, J. Hua and M. Ouyang, *J. Power Sources*, **226**, 272 (2013).
4. S.-W. Kang, H.-M. Xie, W. Zhang, J.-P. Zhang, Z. Ma, R.-S. Wang

and X.-L. Wu, *Electrochim. Acta*, **176**, 604 (2015).
5. T. Kubo, K. Fujishima and N. Yamamoto, U.S. Patent, 5,326,455 (1994).
6. N. Takahashi and Y. Hirasawa, U.S. Patent, 20,020,015,833 (2001).
7. C.-C. Lin, C.-H. Yen, S.-C. Lin, C.-C. Hu and W.-P. Dow, *J. Electrochem. Soc.*, **164**, D810 (2017).
8. S. K. Cho, M. J. Kim, H.-C. Koo, O. J. Kwon and J. J. Kim, *Thin Solid Films*, **520**, 2136 (2012).
9. H. C. Kim, M. J. Kim, S. Choe, T. Lim, K. J. Park, K. H. Kim, S. H. Ahn, S.-K. Kim and J. J. Kim, *J. Electrochem. Soc.*, **161**, D749 (2014).
10. H. C. Kim, M. J. Kim, T. Lim, K. J. Park, K. H. Kim, S. Choe, S.-K. Kim and J. J. Kim, *Thin Solid Films*, **550**, 421 (2014).
11. P.-F. Chan, R.-H. Ren, S.-I. Wen, H.-C. Chang and W.-P. Dow, *J. Electrochem. Soc.*, **164**, D660 (2017).
12. M. Hakamada, Y. Nakamoto, H. Matsumoto, H. Iwasaki, Y. Chen, H. Kusuda and M. Mabuchi, *Mater. Sci. Eng. A*, **457**, 120 (2007).
13. D. Xu, W.L. Kwan, K. Chen, X. Zhang, V. Ozoliņš and K. N. Tu, *Appl. Phys. Lett.*, **91**, 254105 (2007).
14. L. Lu, Y. Shen, X. Chen, L. Qian and K. Lu, *Science*, **304**, 422 (2004).
15. L. Lu, X. Chen, X. Huang and K. Lu, *Science*, **323**, 607 (2009).
16. K. Lu, L. Lu and S. Suresh, *Science*, **324**, 349 (2009).
17. M. J. Kim, S. K. Cho, H.-C. Koo, T. Lim, K. J. Park and J. J. Kim, *J. Electrochem. Soc.*, **157**, D564 (2010).
18. M. J. Kim, T. Lim, K. J. Park, S. K. Cho, S.-K. Kim and J. J. Kim, *J. Electrochem. Soc.*, **159**, D538 (2012).
19. M. J. Kim, T. Lim, K. J. Park, O. J. Kwon, S.-K. Kim and J. J. Kim, *J. Electrochem. Soc.*, **159**, D544 (2012).
20. X. Chen and L. Lu, *Scrip. Mater.*, **57**, 133 (2007).
21. G.-T. Lui, D. Chen and J.-C. Kuo, *J. Phys. D: Appl. Phys.*, **42**, 215410 (2009).
22. V. A. Vas'Ko, I. Tabakovic, S. C. Riemer and M. T. Kief, *Microelectron. Eng.*, **75**, 71 (2004).
23. D. S. Stoychev, I. V. Tomov and I. B. Vitanova, *J. Appl. Electrochem.*, **15**, 879 (1985).
24. S. Mizumoto, H. Nawafune, T. Hiroo and M. Haga, *J. Surf. Finish. Soc. Jpn.*, **44**, 687 (1993).
25. H. Nawafune Y. Fukuda, S. Mizumoto and M. Haga, *J. Surf. Finish. Soc. Jpn.*, **46**, 834 (1995).
26. J. M. E. Harper, C. Cabral Jr., P. C. Andricacos, L. Gignac, I. C. Noyan, K. P. Rodbell and C. K. Hu, *J. Appl. Phys.*, **86**, 2516 (1999).
27. V. A. Vas'Ko, I. Tabakovic and S. C. Riemer, *Electrochem. Solid-State Lett.*, **6**, C100 (2003).
28. C.-H. Lee and C.-O. Park, *Jpn. J. Appl. Phys.*, **42**, 4484 (2003).
29. M. Stangl, J. Acker, V. Dittel, W. Gruner, V. Hoffmann and K. Wetzig, *Microelectron. Eng.*, **82**, 189 (2005).
30. E. Shinada, T. Nagoshi, T.-F. M. Chang and M. Sone, *Mater. Sci. Semicond. Process*, **16**, 633 (2013).
31. C.-E. Ho, C.-C. Chen, M.-K. Lu, Y.-W. Lee and Y.-S. Wu, *Surf. Coat. Technol.*, **303**, 86 (2016).
32. C.-C. Chen, C.-H. Yang, Y.-S. Wu and C.-E. Ho, *Surf. Coat. Technol.*, **320**, 489 (2017).
33. M. Matsuda, T. Takahashi, S. Yoshihara and M. Dobashi, *Trans. Jap. Electron. Packaging*, **2**, 55 (2009).
34. M.-Y. Cheng, K.-W. Chen, T.-F. Liu, Y.-L. Wang and H.-P. Feng, *Thin Solid Films*, **518**, 7468 (2010).
35. M. Stangl and M. Militzer, *J. Appl. Phys.*, **103**, 113521 (2008).
36. M. Hasegawa, Y. Nonaka, Y. Negishi, Y. Okinaka and T. Osaka, *J. Electrochem. Soc.*, **153**, C117 (2006).
37. T. Osaka, N. Yamachika, M. Yoshino, M. Hasegawa, Y. Negishi and Y. Okinaka, *Electrochem. Solid-State Lett.*, **12**, D15 (2009).
38. S. Nakahara, S. Ahmed and D. N. Buckley, *Electrochem. Solid-State Lett.*, **10**, D17 (2007).
39. T. Surholt and Chr. Herzig, *Acta Mater.*, **45**, 3817 (1997).
40. N. Hansen and B. Ralph, *Acta Metall.*, **30**, 411 (1982).
41. J. E. Flinn, D. P. Field, G. E. Korth, T. M. Lillo and J. Macheret, *Acta Mater.*, **49**, 2065 (2001).
42. J. W. Hutchinson, *Proc. Roy. Soc. Lond. A.*, **319**, 247 (1970).
43. M. T. Kiser, F. W. Zok and D. S. Wilkinson, *Acta Mater.*, **44**, 3465 (1996).
44. C.-W. Nan and D. R. Clarke, *Acta Mater.*, **44**, 3801 (1996).
45. C.-W. Nan, R. Birringer and H. Gleiter, *Scrip. Mater.*, **37**, 969 (1997).
46. L. Peng, F. Liu, J. Ni and X. Lai, *Mater. Des.*, **28**, 1731 (2007).